Molecularly Imprinted Synthetic Glucosidase for the Hydrolysis of Cellulose in Aqueous and Nonaqueous Solutions

Xiaowei Li, Milad Zangiabadi, and Yan Zhao*

Department of Chemistry, Iowa State University, Ames, Iowa 50011-3111

ABSTRACT: Molecular imprinting is a powerful and yet simple method to create multifunctional binding sites within a cross-linked polymer network. We report a new class of synthetic glucosidase prepared through molecular imprinting and postfunctionalization of cross-linked surfactant micelles. These catalysts are protein-sized water-soluble nanoparticles that can be modified in multiple ways. As their natural counterparts, they bind a glucose-containing oligo- or polysaccharide. They contain acidic groups near the glycosidic bond to be cleaved, with the number and distance of the acid groups tuned systematically. Hydrolysis of cellulose in a key step in biomass conversion but is hampered by the incalcitrance of the highly crystalline cellulose fibers. The synthetic glucosidases are shown to hydrolyze cellobiose and cellulose under a variety of conditions. The best catalyst, with a biomimetic double acid catalytic motif, can hydrolyze cellulose with one fifth of the activity of commercial cellulases in aqueous buffer. As a highly cross-linked polymeric nanoparticle, the synthetic catalyst is stable at elevated temperatures in both aqueous and nonaqueous solvents. In a polar aprotic solvent/ionic liquid mixture, it hydrolyzes cellulose several times faster than commercial cellulases in aqueous buffer. When deposited on magnetic nanoparticles, it retains 75% of its activity after 10 cycles of usage.

INTRODUCTION

The extraordinary catalytic efficiency and selectivity of enzymes have motivated generations of scientists to develop synthetic mimics with similar capabilities.[1-3] Although chemists rightfully argue that enzymes are "not different, just better" than synthetic catalysts,[4] artificial enzymes created on purely synthetic or semi-natural platforms generally do not match their natural counterparts in performance.[1-3] The deficiency of artificial enzymes has many reasons. Apart from a detailed understanding of enzymatic activity, a large roadblock is the lack of suitable synthetic strategies to construct multifunctional active sites with accurately positioned catalytic groups for substrates with complex structures and shapes.

A powerful method to create multifunctional binding sites for molecules of many different sizes is molecular imprinting.[5-7] In its traditional embodiment, template molecules are mixed with a large amount of cross-linkers and functional monomers (FMs) that can interact with the templates by noncovalent or reversible covalent bonds. Free radical polymerization, followed by template removal, yields a highly cross-linked polymeric network with embedded imprinted sites complementary to the templates ideally in size, shape, and distribution of functional groups. Owing to simplicity of the preparation and broad utility to molecules of different types, molecularly imprinted polymers (MIPs) have found numerous applications in biomedical research[8,9] and catalysis.[10-16]
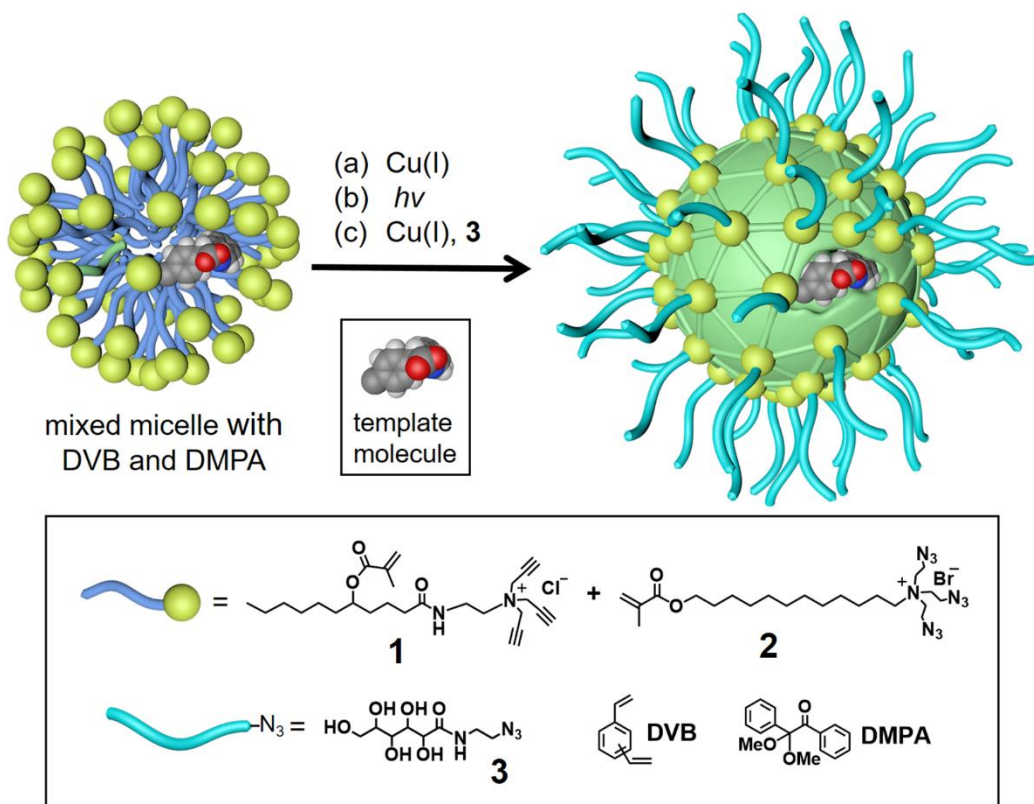
To create a catalytic active site similar to those found in enzymes, one needs not only high fidelity in the imprinting process but also abilities to postmodify the imprinted site to introduce catalytic groups that could not be introduced directly through functional monomers during the initial imprinting. In recent years, our group has developed a method to molecularly imprint surfactant micelles.[17] The nanoconfinement of the polymerization and cross-linking within the surface-cross-linked micelle yield an extraordinary templating effect,[18] with the imprint/nonimprint ratio in binding (i.e., imprinting factor) frequently reaching hundreds[19] and sometimes 10,000.[20] The addition,[18] removal,[18] and shift[21] of a single methyl (or methylene) group in the guest can be distinguished by the so-called molecularly imprinted nanoparticles (MINPs). Catalytic groups can be installed inside the imprinted pockets to afford highly-selective, enzyme-mimetic catalysts.[22-25]

In this work, we report MINP-based synthetic glucosidases for the hydrolysis of cellulose, taking advantage of the high fidelity of micellar imprinting and facile postfunctionalization enabled by the accessibility of the imprinted sites. Cellulose constitutes 35–50% of lignocellulosic biomass and is an abundant carbon-neutral natural resource.[26-28] Whether for chemical or fuel production, it first has to be depolymerized into soluble monomeric and oligomeric sugars, usually through catalytic hydrolysis. Although natural enzymes (i.e., cellulases) exist for this process,[29] the easily denatured protein structure limits the operating window of these enzymes and makes their recycling difficult. In recent years, great efforts have been devoted toward improving the stability of cellulases[30,31] but high temperatures and nonaqueous solvents are inherently difficult for any enzyme-based catalysts. In contrast, our polymer-based synthetic glucosidases were shown to tolerate elevated temperatures, nonaqueous solution, and extreme pH conditions. Additionally, they could be easily "clicked" onto magnetic nanoparticles to be converted into a heterogeneous catalyst that retained 75% of its activity after 10 cycles of usage.

RESULTS AND DISCUSSION

Preparation of Synthetic Glucosidase and Its Hydrolysis of Cellobiose. Carbohydrates can be bound by boronic acids[32-35] or boroxole[36-39] via reversible boronate bonds formed with specific 1,2-

Scheme 1. General procedure for the MINP preparation from mixed micelle of **1** and **2** containing DVB and DMPA.

and 1,3-diols on the sugar. The glycosidic linkages in cellulose are essentially acid-sensitive acetals. Thus, to hydrolyze cellulose, a synthetic cellulase needs to bind a portion of the polymer chain and have an acidic group right next to the glycosidic bond to be cleaved.

Our construction of such a catalyst was based on molecular imprinting[5-7] in cross-linked micelles (Scheme 1).[17,35,39] This method starts with spontaneous formation of mixed micelles of **1** and **2** containing a template molecule, divinylbenzene (DVB, a free radical cross-linker), and 2,2-dimethoxy-2-phenylacetophenone (DMPA, a photoinitiator). Cu(I) catalysts are used to cross-link the surface of the micelle by the highly efficient alkyne–azide "click" reaction, facilitated additionally by the proximity of the reactive groups. UV-induced free-radical polymerization then cross-links the micelle core around the template, and a second round click reaction between **3** and the residual alkynes on the micelle installs a layer of hydrophilic ligand on the surface. The surface ligands enable the resulting MINPs to be purified by simple precipitation and washing with organic solvents, with the template molecules removed during the process. A surfactant/template ratio of 50 is commonly used to give an average of one binding site per nanoparticle, since MINP contains ~50 cross-linked surfactants.[17]

The most challenging aspect of building a synthetic enzyme is probably accurate positioning of multiple catalytic groups near the bonds to be transformed.[1-3] For this purpose, we designed template **5**, consisting of a glucose and an aglycon containing a reversible imine bond (Scheme 2). It reacted with vinylphenylboroxole **4** *in situ* in the micellar solution to afford amphiphilic, anionic template–FM complex **6**, which was stabilized by the cationic micelle.[36,38-40] The resulting MINP(**5**) had the template covalently polymerized into the micellar core due to the vinyl group on the template. The

imine bound was hydrolyzed by 6 N hydrochloric acid at 95 °C to give MINP-CHO(**5**). The aldehyde group in the active site was further derivatized with amino acids **8a–i** via reductive amination following previously established protocols[39,41,42] to afford MINP (**5+8a–i**) as our synthetic glucosidase. The cross-linking and formation of MINPs generally can be characterized by a combination of ¹H NMR spectroscopy (Figures S1–2), dynamic light scattering (Figures S3–4), and transmission electron microscopy (Figure S5).

As shown in Scheme 2, MINP (**5+8a–i**) has a boroxole group in the active site to bind the terminal glucose of cellobiose (or cellulose), with an acid positioned near the glycosidic bond to catalyze the hydrolysis. Boronate **6** has two free hydroxyl groups and its amphiphilicity helps itself to be anchored near the surface of the micelle—a feature important to the removal of the template to vacate the imprinted site after micellar imprinting.[17] In the final catalyst, it is also important to keep the active site close to the surface so that the unbound glucose residues of the substrate can stay in solution while the terminal glucose engages in reversible boronate formation with the boroxole inside the active site.

Amino acids **8a–i** allowed the introduction of different acids in the active site, with its flexibility and distance to the glycosidic bond tuned systematically. To our delight, the resulting MINP(**5+8a–i**) hydrolyzed cellobiose, our model substrate, in a 21–64% yield at 60 °C and in pH 6 buffer (Table 1, entries 1–7). It is interesting that **8a**, which was similar in dimension to the part of the aryl aglycon of **5** removed by imine hydrolysis, yielded a less active catalyst than **8d**. A tightly fit active site thus seems less efficient than one with some flexibility. When the number of methylene groups (n = 3) stayed the same with **8d**, **8h**, and **8i**, the most acidic sulfonic acid gave the fastest hydrolysis.
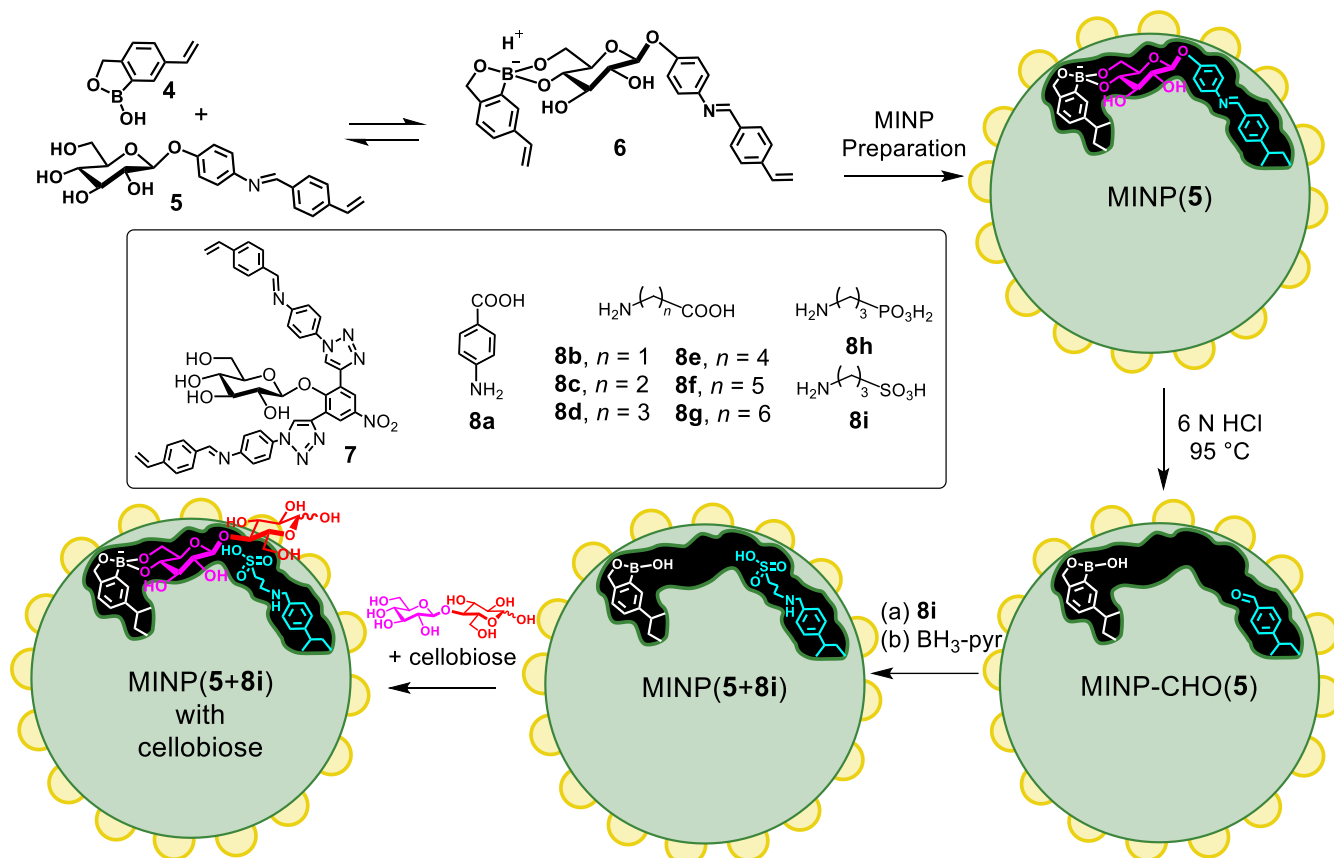
Scheme 2. Preparation of MINP-based synthetic glycosidase, with a schematic representation of the active site functionalized with **8i** and a cellobiose bound by the boroxole group introduced through FM **4**. The surface ligands are omitted for clarity.

Table 1. Hydrolysis of cellobiose catalyzed by MINPs in 10 mM MES buffer (pH 6).[a]

Entry	catalysts	temp. (°C)	yield (%)
1	MINP(**5+8a**)	60	42 ± 6
2	MINP(**5+8b**)	60	22 ± 4
3	MINP(**5+8c**)	60	25 ± 4
4	MINP(**5+8d**)	60	51 ± 7
5	MINP(**5+8e**)	60	21 ± 4
6	MINP(**5+8h**)	60	57 ± 4
7	MINP(**5+8i**)	60	64 ± 8
8	MINP(**5+8i**)	90	74 ± 6
9	MINP(**7+8c**)	60	0
10	MINP(**7+8d**)	60	17 ± 2
11	MINP(**7+8e**)	60	54 ± 6
12	MINP(**7+8f**)	60	94 ± 4
13	MINP(**7+8g**)	60	77 ± 8
14	MINP(**7+8f**)	90	98 ± 1
15	NINP with **8f**[b]	60	0
16	**8i**	60	~2
17	**8f**	60	~1
18	*none*	60	0

[a] Reactions were performed with 0.2 mM of cellobiose and 20 μM of catalysts in 1.0 mL MES buffer (10 mM, pH = 6.0) for 24 h. Yields were determined by LC-MS using standard curves generated from authentic samples. [b] NINP was nonimprinted nanoparticle prepared with 1 equiv FM **4** but without any template.

The above method was not limited to a monoacidic design. A huge number of glycosidases exist in nature to cleave the glycosidic bonds of oligo- and polysaccharides.[43] A highly conserved feature of these enzymes is a pair of carboxylic acids in the active site—a remarkably simple catalytic motif. The hydrolytic mechanism involves one carboxylic acid as a general acid to protonate the glycosidic oxygen. For inverting glycosidases, the other carboxyl 7–11 Å apart, in the deprotonated form, is a general base to deprotonate the attacking water nucleophile. For retaining glycosidases, the other carboxylate (~5 Å apart) is the attacking nucleophile.[43]

To create a similar feature in our synthetic glucosidase, we synthesized template **7** with two imine bonds, which allowed two acids to be installed in the active site, sandwiching the glycosidic bond in the final structure (Scheme 2). Gratifyingly, the optimized diacidic catalyst, i.e., MINP(**7+8f**), hydrolyzed cellobiose significantly better (94% yield at 60 °C) than the best monoacidic MINP(**5+8i**), despite the more acidic sulfonic acid in the latter (Table 1). The activity, once again, can be tuned by the distance of the acids. Control experiments indicated that nonimprinted nanoparticles (NINPs) were ineffective and the background hydrolysis was low with or without the acid additives (entries 15–18). Note that MINP(**5+8i**) and MINP(**7+8f**) required different lengths of tethers to connect the acidic groups. The longer tether (n = 5) required for MINP(**7+8f**) is reasonable given the longer distance between the imine group and the exocyclic glycosidic oxygen in the template.

Table 2. ITC binding data for sugar guests by MINPs.[a]

Entry	MINP	guest	pH	K_a ($\times 10^3$ M^{-1})	ΔG (kcal/mol)	N
1	MINP-CHO(**5**)	glucose	7.4	8.85 ± 0.68	-5.38	1.03 ± 0.03
2	MINP(**5+8i**)	glucose	7.4	9.07 ± 0.86	-5.40	0.83 ± 0.09
3	MINP-CHO(**7**)	glucose	7.4	17.40 ± 1.92	-5.78	1.01 ± 0.03
4	MINP(**7+8f**)	glucose	7.4	22.60 ± 1.07	-5.94	0.91 ± 0.03
5	MINP(**5+8i**)	glucose	6.0	7.52 ± 0.79	-5.28	0.95 ± 0.07
6	MINP(**5+8i**)	cellobiose	6.0	5.71 ± 0.51	-5.12	0.78 ± 0.08
7	MINP (**7+8f**)	glucose	6.0	15.70 ± 1.32	-5.72	0.79 ± 0.09
8	MINP (**7+8f**)	cellobiose	6.0	6.98 ± 1.52	-5.24	1.06 ± 0.17
9	NINP[b]	glucose	7.4	< 0.05[b]	--[b]	--[b]

[a] The FM/template ratio in the MINP synthesis was 1:1 unless otherwise indicated. The cross-linkable surfactants were a 3:2 mixture of **1** and **2**. The titrations were performed in 10 mM HEPES buffer at pH 7.4 and 10 mM MES buffer at pH 6 at 298 K. The ITC titration curves are reported in the Figures S6-14, including the binding enthalpy and entropy. N is the average number of binding site per nanoparticle measured by ITC. [b] The particle was prepared with 1.0 equiv. FM **4** but without any template. Because the binding constant was estimated from ITC, -ΔG and N are not listed.

Both the intermediate aldehyde-containing MINP-CHOs and the final catalysts bound glucose in aqueous buffer, with a binding constant (K_a) of 7–23 × 10^3 M^{-1} determined from isothermal titration calorimetry (ITC) (Table 2). The binding affinity matched those for monosaccharides by natural lectins (K_a = 10^3–10^4 M^{-1}).[44] Binding for cellobiose was slightly weaker than for glucose and a decrease of pH from 7.4 to 6.0—the pH for the cellobiose hydrolysis experiments in Table 1—weakened the binding slightly. Molecular imprinting was key to the binding, as the nonimprinted nanoparticles (NINPs) prepared with **4** in the absence of template showed negligible binding. The MINP/NINP binding ratio (i.e., the imprinting factor) for glucose was >450 for MINP(**7+8f**).

Catalytic Behavior of MINP Catalysts in the Hydrolysis of Cellobiose. MINP(**5+8i**) and MINP(**7+8f**), our best mono- and diacid catalysts, showed different pH profiles in their hydrolysis of cellobiose (Figure 1). The mono-sulfonic acid catalyst displayed an increase of activity upon decreasing solution pH all the way to pH 4.5, where the peak activity was reached. Its overall preference for acidic conditions can be understood from the following two considerations.
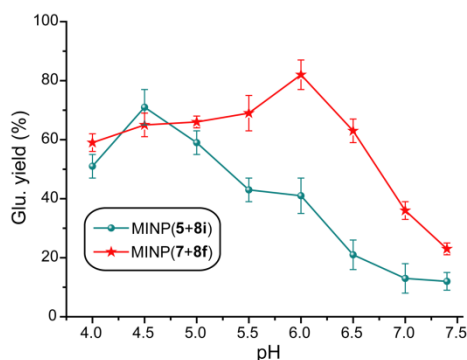

Figure 1. Effects of solution pH on the hydrolysis of cellobiose by MINP(**5+8i**) and MINP(**7+8f**). Reactions were performed with 0.2 mM of cellobiose and 20 μM of MINP in 1.0 mL buffer (10 mM) at 37 °C for 24 h. Yields were determined by LC-MS using standard curves generated from authentic samples. NaOAc buffer was used for pH 4.0–5.0, MES buffer for pH 5.5–6.5, and HEPES buffer for pH 7.0–7.4.

First, to be useful in an acid-catalyzed hydrolysis of acetal,[45] the sulfonic acid in the active site of MINP(**5+8i**) needs to be able to donate a proton to the glycosidic oxygen and thus be protonated prior to substrate binding. The pK_a of the sulfonic acid in 2-aminoethanesulfonic acid is 1.5 in an aqueous solution[46] but the microenvironment of an acid (or base) is known to strongly influence its strength. For example, the ammonium side chain of lysine has a pK_a of 10.5 in water but the value decreases to 5.6 in the active site of acetoacetate decarboxylase.[47] The shift often results from a combination of hydrophobic effect[48] and ionic interactions.[49] The former destabilizes ionic species and increases the pK_a of a neutral acid (e.g., sulfonic or carboxylic acid) but decreases the pK_a of a charged acid such as ammonium. As for the electrostatic interactions, vicinal positive charges generally make protonation of a base more difficult and deprotonation of an acid easier. A recent work of ours shows that 1-pyrenesulfonic acid has a pK_a of ca. 7 inside a MINP pocket.[50] In the case of MINP(**5+8i**), the overall increase of hydrolytic activity over pH 7.4–4.5 suggests that the pK_a of its sulfonic acid should be lower than 7.

Second, in order for the MINP catalyst to hydrolyze cellobiose efficiently, the boroxole group needs to bind the terminal glucose from the nonreducing end. Benzoboroxole has a pK_a of 7.3[51] and the strongest binding (for fructose) occurs at ~pH 7.4, very close to the pK_a value.[40] Inside the MINP, the anionic form of the boroxole–sugar complex (shown in Scheme 2) can be stabilized by the cationic headgroups of the cross-linked surfactants,[38] and the acid–base equilibrium of boroxole also strongly depends on environmental polarity.[40] Nonetheless, our ITC data in Table 2 clearly shows that binding for guest guests become weaker at lower pH for both MINP(**5+8i**) and MINP(**7+8f**).

The overall pH profile of the MINP-catalyzed hydrolysis, hence, should reflect a trade-off between the above two effects: hydrolysis is favored by acidic conditions but binding of the substrate prefers a neutral pH. Interestingly, although MINP(**5+8i**) and MINP(**7+8f**) both seemed to experience such a trade-off, the optimal pH for the dicarboxylic acid catalyst was significantly higher, at pH 6.0 instead of 4.5 (Figure 1). The increase is reasonable given that (a) a carboxylic acid has a higher pK_a than a sulfonic acid, at least in an aqueous solution, and (b) the cooperative catalysis of the two carboxylic acids in natural glycosidases requires one acid to be protonated and another one deprotonated.[43] A similar mechanism should be followed by MINP(**7+8f**) given its high catalytic activity and sensitivity in the tether length (Table 1).

MINP(**5+8i**) and MINP(**7+8f**) displayed Michaelis-Menten

kinetics in the hydrolysis of cellobiose (Figures 2 and 3). MINP($\mathbf{5}$+$\mathbf{8i}$) had a k_{cat} value of 0.027 min^{-1} and K_m of 0.74 mM in pH 6 buffer at 60 °C. MINP($\mathbf{7}$+$\mathbf{8f}$) had an experimentally comparable K_m value and a turnover 3.2-times faster than the monoacidic MINP. The rate constant for cellobiose hydrolysis in acidic water is estimated from a modified Saeman equation to be ~ 4.9×10^{-10} s^{-1} at pH 6 and 60 °C.[52] Thus, a rate acceleration of ca. 9×10^5 and 3×10^6 was achieved by MINP($\mathbf{5}$+$\mathbf{8i}$) and MINP($\mathbf{7}$+$\mathbf{8f}$), respectively, over *acid-catalyzed* hydrolysis in aqueous solution at pH 6. Clearly, positioning the acidic groups at the glycosidic bond is hugely beneficial to the catalyzed hydrolysis.
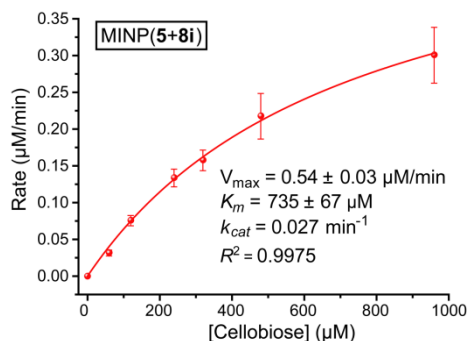

Figure 2. Michaelis-Menten plot for the hydrolysis of cellobiose by MINP($\mathbf{5}$+$\mathbf{8i}$) in MES buffer (10 mM, pH = 6.0) at 60 °C. [MINP($\mathbf{5}$+$\mathbf{8i}$)] = 20.0 μM.

Figure 3. Michaelis-Menten plot for the hydrolysis of cellobiose by MINP($\mathbf{7}$+$\mathbf{8f}$) in MES buffer (10 mM, pH = 6.0) at 60 °C. [MINP($\mathbf{7}$+$\mathbf{8f}$)] = 10.0 μM.

A great many wild-type and engineered β-glucosidases have been reported in the literature, showing a broad range of catalytic activities in cellobiose hydrolysis.[53,54] The catalytic efficiency of the diacidic MINP($\mathbf{7}$+$\mathbf{8f}$) (k_{cat}/K_m =132 M^{-1} min^{-1}) was roughly 1/14th of that of digestive β-glucosidase GH1 (a relatively slow enzyme) from *Spodoptera frugiperda* (k_{cat}/K_m = 1780 M^{-1} min^{-1}, k_{cat} = of 5.7 min^{-1} and K_m = 3.2 mM).[55] In comparison to the natural β-glucosidase, MINP($\mathbf{7}$+$\mathbf{8f}$) had a lower catalytic turnover but significantly stronger binding for the substrate.

Hydrolysis of Cellulose in Aqueous and Nonaqueous Solution. Encouraged by the facile hydrolysis of cellobiose by the synthetic glucosidases, we attempted their hydrolysis of cellulose, a much more challenging substrate due to its highly crystalline nature. The initial tests involved hydrolysis in aqueous buffer, following established procedures to measure enzyme activity.[31] For comparison purposes, we used a commercial cellulase isolated from *Aspergillus niger*, which is an endocellulase active on both cellulose and related oligomers.[56] A well-established spectrophotometric assay was used to monitor the hydrolysis of type 20 Sigmacell cellulose powder (Figure S17).[31,57] The method measures all reducing sugars formed even though liquid chromatography–mass spectrometry (LC-MS) indicated that glucose was the dominant product (Figure S18).

Table 3 compares the hydrolytic properties of MINP($\mathbf{7}$+$\mathbf{8f}$) and cellulase from *Aspergillus niger* under a variety of conditions. For the natural enzyme, an increase in the catalyst's concentration lowered the observed enzyme activity from 0.200 to 0.107 μmol mg^{-1} h^{-1} (Table 3, entries 2, 4, and 6). This result is reasonable because many cellulases operate through a processive mechanism in which the enzyme hydrolyzes a cellulose chain while decrystalizing it from cellulose crystals.[29,58] To do this, the enzyme has a tunnel (e.g., cellobiohydrolases) or deep cleft (e.g., endoglucanases) that binds a cellulose chain sometimes with over 20 kcal/mol binding energy.[59] Often a trade-off between processivity and hydrolytic rate is observed that derives from the binding.[60] Since only the cellulose chains on the surface of the crystals can react with these enzymes, once the surface is saturated with a strongly binding cellulase, adding additional enzymes will not increase the hydrolytic rate and will decrease the observed average enzyme activity measured from the formation of reducing sugars.

Table 3. Hydrolysis of cellulose by cellulases and MINP($\mathbf{7}$+$\mathbf{8f}$).[a]

entry	catalysts	catalyst concentration (mg/ml)	solvent	temp (°C)	[reducing sugar] (mg/mL)	enzyme activity (μmol mg^{-1} h^{-1})	relative activity (enzyme/MINP)
1	MINP($\mathbf{7}$+$\mathbf{8f}$)	1.0	pH 5 NaOAc buffer	37	0.015 ± 0.002	0.007 ± 0.001	29
2	cellulases	1.0	pH 5 NaOAc buffer	37	0.43 ± 0.03	0.200 ± 0.011	--
3	MINP($\mathbf{7}$+$\mathbf{8f}$)	2.0	pH 5 NaOAc buffer	37	0.07 ± 0.01	0.017 ± 0.007	9
4	cellulases	2.0	pH 5 NaOAc buffer	37	0.68 ± 0.35	0.158 ± 0.021	--
5	MINP($\mathbf{7}$+$\mathbf{8f}$)	5.0	pH 5 NaOAc buffer	37	0.25 ± 0.04	0.024 ± 0.004	4.5
6	cellulases	5.0	pH 5 NaOAc buffer	37	1.15 ± 0.21	0.107 ± 0.019	--
7	MINP($\mathbf{7}$+$\mathbf{8f}$)	5.0	pH 5 NaOAc buffer	60	0.43 ± 0.08	0.039 ± 0.008	0.56
8	cellulases	5.0	pH 5 NaOAc buffer	60	0.24 ± 0.03	0.022 ± 0.003	--
9	MINP($\mathbf{7}$+$\mathbf{8f}$)	5.0	pH 5 NaOAc buffer	90	0.79 ± 0.13	0.073 ± 0.012	0
10	cellulases	5.0	pH 5 NaOAc buffer	90	0	0	--
11	MINP($\mathbf{7}$+$\mathbf{8f}$)	5.0	83% H$_3$PO$_4$	37	0.71 ± 0.33	0.067 ± 0.031	0
12	cellulases	5.0	83% H$_3$PO$_4$	37	0	0	--

[a] The reactions were performed in duplicates with [cellulose] = 5.0 mg/mL in 1.0 mL 10 mM NaOAc buffer (pH 5) for 12 h unless indicated otherwise.

Table 4. Hydrolysis of cellulose by MINP(**5**+**8i**) and MINP(**7**+**8f**) in mixtures of ionic liquids and a polar aprotic solvent.[a]

entry	catalyst	solvent	temp. (°C)	[reducing sugar] (mg/mL)	enzyme activity (μmol mg^{-1} h^{-1})
1	MINP(**5**+**8i**)	[C$_4$mim]Cl	90	0.44 ± 0.05	0.051 ± 0.006
2	MINP(**5**+**8i**)	1:1 [C$_4$mim]Cl/DMF	90	1.33 ± 0.17	0.154 ± 0.019
3	MINP(**5**+**8i**)	1:1 [C$_4$mim]Cl/DMSO	90	2.24 ± 0.14	0.258 ± 0.016
4	MINP(**5**+**8i**)	1:1 [C$_4$mim]Cl/DMSO	110	2.87 ± 0.21	0.329 ± 0.024
5	MINP(**5**+**8i**)	1:1 [C$_4$mim]Cl/DMSO	130	3.41 ± 0.33	0.391 ± 0.038
6	MINP(**7**+**8f**)	[C$_4$mim]Cl	90	0.21 ± 0.04	0.024 ± 0.005
7	MINP(**7**+**8f**)	9:1 [C$_4$mim]Cl/DMSO	90	1.17 ± 0.14	0.135 ± 0.016
8	MINP(**7**+**8f**)	8:2 [C$_4$mim]Cl/DMSO	90	1.41 ± 0.08	0.163 ± 0.009
9	MINP(**7**+**8f**)	7:3 [C$_4$mim]Cl/DMSO	90	1.98 ± 0.21	0.229 ± 0.024
10	MINP(**7**+**8f**)	6:4 [C$_4$mim]Cl/DMSO	90	2.87 ± 0.17	0.332 ± 0.020
11	MINP(**7**+**8f**)	5:5 [C$_4$mim]Cl/DMSO	90	4.17 ± 0.37	0.480 ± 0.043
12	MINP(**7**+**8f**)	5:5 [C$_4$mim]Cl/DMSO	110	4.51 ± 0.44	0.519 ± 0.051
13	MINP(**7**+**8f**)	5:5 [C$_4$mim]Cl/DMSO	130	4.97 ± 0.61	0.572 ± 0.071
14	MINP(**7**+**8f**)	5:5 [C$_4$mim]Cl/DMSO[b]	90	5.92 ± 0.11	0.431 ± 0.014
15	MINP(**7**+**8f**)	5:5 [C$_4$mim]Cl/DMSO[c]	90	6.76 ± 0.32	0.197 ± 0.011
16	MINP(**7**+**8f**)	4:6 [C$_4$mim]Cl/DMSO[d]	90	1.55 ± 0.11	0.179 ± 0.013
17	MINP(**7**+**8f**)	5:5 [C$_4$mim]Cl/DMSO+5% H$_2$O	90	5.41 ± 0.41	0.623 ± 0.047
18	MINP(**7**+**8f**)	1:9 [C$_2$mim]OAc/DMSO	90	5.87 ± 0.24	0.676 ± 0.028
19	MINP(**7**+**8f**)	1:9 [C$_2$mim]OAc/DMSO[b]	90	6.94 ± 0.15	0.504 ± 0.021
20	MINP(**7**+**8f**)	1:9 [C$_2$mim]OAc/DMSO[c]	90	7.24 ± 0.18	0.211 ± 0.035
21	MINP(**7**+**8f**)	2:8 [C$_2$mim]OAc/DMSO+5% H$_2$O	90	6.25 ± 0.58	0.719 ± 0.067

[a]The reactions were performed in duplicates with [cellulose] = 8.0 mg/mL and [MINP] = 2.0 mg/mL in 0.5 mL of solvent for 24 h. [b] [MINP] = 3.2 mg/mL. [c] [MINP] = 8.0 mg/mL. [d] Cellulose dissolved partially in this mixture.

MINP(**7**+**8f**) clearly did not have such an ability. The same increase of its concentration displayed an opposite trend and steadily *increased* the observed enzyme activity, from 0.007 to 0.024 μmol mg^{-1} h^{-1} (Table 3, entries 1, 3, and 5). This is not surprising because the binding free energy for glucose and cellobiose by the synthetic glucosidase was only 5–6 kcal/mol (Table 2), far lower than those of common cellulases. Under our experimental conditions, the steady increase of the observed enzyme activity suggests that the surface is far from being saturated by the MINP catalyst, even at 1:1 weight ratio of cellulose and the catalyst. Because the repeat unit in a cellulose polymer has a molecular weight of 162 Da and the MINP (with an average of one active site per nanoparticle) ~50,000, the substrate/catalyst ratio was 300 to 1,500 under our experimental conditions.

Despite its lack of a processive mechanism, MINP(**7**+**8f**) showed activities that actually can be compared with those of natural cellulase: the enzyme/MINP ratio in Table 3 decreased steadily from 29 all the way to 4.5 with an increase of catalyst concentration (entries 1–6). Even if the activity of the enzyme at low concentration is compared with the activity of the MINP at high concentration (entries 1 and 5), the difference was a factor of 8.3.

One notable strength of the synthetic glucosidase was its stability, due to its highly cross-linked nature. While the natural cellulase continued to lose activity as the reaction temperature increased from 37 to 60 and then to 90 °C in the pH 5 buffer, MINP(**7**+**8f**) became more efficient, with its activity at 90 °C (0.073 μmol mg^{-1} h^{-1}) reaching nearly 70% of that of cellulases (0.107 μmol mg^{-1} h^{-1}) at 37 °C at the same concentration of catalyst. The robustness of the MINP catalysts was also shown by its ability to hydrolyze cellulose in 83% phosphoric acid, which dissolved cellulose completely[61] but inactivated the natural enzymes. The synthetic catalyst was nearly 3 times more active in this extremely acidic condition than in pH 5 buffer at the same temperature of 37 °C.

Ionic liquids such as 1-butyl-3-methylimidazolium chloride ([C$_4$mim]Cl) have a tremendous ability to dissolve cellulose[62,63] and are known to facilitate the acid-catalyzed hydrolysis of cellulose.[64-66] Unfortunately, enzymes have poor stability and low activity in ionic liquids, especially at elevated temperatures.[30] In contrast, the extraordinary stability of the MINP-based artificial enzymes allowed the hydrolysis to be performed under conditions totally impossible for natural enzymes.

Table 4 shows that the activity of both MINP(**5**+**8i**) and MINP(**7**+**8f**) improved in ionic liquids as the reaction mixture became homogeneous. A polar aprotic solvent (dimethyl sulfoxide or DMSO) could be added to further speed up the hydrolysis as long as the reaction mixture stayed homogeneous.[67] The solvent effect in the ionic liquids/DMSO mixtures followed a trend opposite to that observed in cellulose hydrolysis catalyzed by *p*-toluenesulfonic acid (*p*-TSA). Hydrolysis of cellulose (and also cellobiose) is reported to become faster with a higher fraction of ionic liquids in the binary solvent mixture for the small acid catalyst, as a result of increased Hammett acidity of *p*-TSA by the ionic liquids.[68] For our MINP catalysts, an increase of acidity first is not expected to be as useful, because the more acidic, monosulfonic acid MINP(**5**+**8i**) was less active than the less acidic, dicarboxylic acid MINP(**7**+**8f**) in aqueous or nonaqueous solutions. Apparently, cooperative catalysis between the carboxylate/carboxylic acid was far more powerful than the "brute force" derived from a single stronger sulfonic acid. Moreover, when the acid groups are located inside the MINP active site, the benefit seen in the solution most likely would not even occur. On the other hand, higher ionic liquids in the binary mixture substantially increases the viscosity of the solution.[68] Diffusion of the 5 nm-sized MINP catalyst thus would become significantly faster as more DMSO is added to the mixture and many have helped the mass transfer and contributed to the higher activity of MINP(**7**+**8f**).

In the 1:1 mixture of [C$_4$mim]Cl/DMSO, the enzyme activity of MINP(**7**+**8f**) reached 0.48 μmol mg^{-1} h^{-1} at 90 °C (Table 4, entry 11), 2.4 times of the best (0.20 μmol mg^{-1} h^{-1}) from the cellulase in

aqueous buffer under our experimental conditions (Table 3, entry 2). An increase of temperature to 130 °C increased the activity of MINP(**7**+**8f**) further to 0.572 µmol mg^{-1} h^{-1} (Table 4, entry 13), underscoring the robustness of the synthetic enzyme. A small amount of water could speed up the reaction even further (Table 4, entry 17; Table S1).

1-Ethyl-3-methylimidazolium acetate ([C$_2$mim]OAc) can dissolve cellulose particularly well in the presence of other organic solvents.[67] In our hands, a 1:9 [C$_2$mim]OAc/DMSO mixture increased the hydrolytic activity of MINP(**7**+**8f**) to 0.676 µmol mg^{-1} h^{-1} (Table 4, entry 18). Notably, in these homogeneous reaction mixtures, increasing the concentration of the MINP catalyst was no longer beneficial and actually decreased the observed enzyme activity (compare entries 11 with 14–15 and also entries 18–20), similar to the trend observed for the cellulase in aqueous reaction. Thus, a high concentration of the MINP catalyst was no longer needed in the ionic liquids/DMSO mixture, possibly because the dissolved polymer chains were already saturated with the MINP at the low catalyst loading. Because the MINP could only bind the nonreducing end of a cellulose chain through boronate bonds, each polymer chain could only accommodate a single catalyst. Also, boronate bonds are labile in water;[40] stronger binding in the more organic ionic liquids/DMSO mixture was not surprising.

Addition of water to the [C$_2$mim]OAc/DMSO mixture required more ionic liquids to keep cellulose homogeneous in the solution. The highest activity achieved by our synthetic glucosidase was 0.719 µmol mg^{-1} h^{-1} in 2:8 [C$_2$mim]OAc/DMSO with 5% H$_2$O, ~3.6 times of the best for the cellulase in aqueous buffer at 37 °C. Ionic liquids generally inactive cellulases[30,69] and indeed inactivated the cellulase from *Aspergillus niger* under our harsh experimental conditions. The best comparison for MINP(**7**+**8f**)—a mimic of β-glucosidase—in the literature is the cationized β-glucosidase reported by Hallet and co-workers, which displayed remarkable stability in ionic liquids.[31] Nonetheless, when the latter was used as the sole catalyst to hydrolyze cellulose in [C$_2$mim]OAc, the observed enzyme activity was <0.1 µmol mg^{-1} h^{-1} at temperatures ranging from 50 to 120 °C.

Figure 4 shows the amount of reducing sugar formed over a period of 24 h at 90 °C from the best monoacidic and diacidic catalysts. We also included the reaction profile for the cellulase from *Aspergillus niger* in aqueous buffer at 37 °C for comparison.
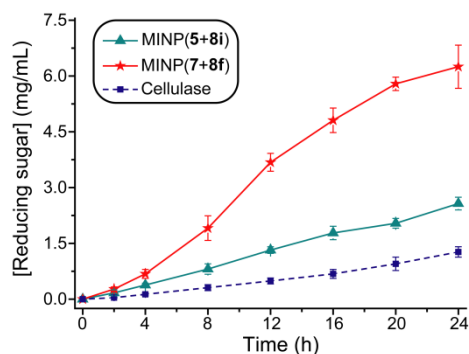

Figure 4. Comparison of reducing sugar formed during hydrolysis of cellulose by the synthetic MINP catalysts in 2:8 [C$_2$mim]OAc/DMSO with 5% H$_2$O at 90 °C and natural cellulase in NaOAc buffer pH 5.0 at 37 °C. [cellulose] =8 mg/mL, [catalyst] = 2 mg/mL.

MINP(**5**+**8i**) and MINP(**7**+**8f**) maintained their activity very well over the extended period of heating (Figure 4). Table 2 shows that both MINPs bound glucose slightly more strongly than cellobiose, at least in aqueous solution. Thus, product inhibition was a concern for these synthetic enzymes, which was also a challenge for natural cellulases.[29] To our delight, no obvious slowdown of the hydrolysis was seen in Figure 4, when the initial slope and those of the later reaction times were compared. MINP contains multiple hydroxylated surface ligands (Scheme 1). It is possible that in the ionic liquids/DMSO mixture a dissolved cellulose chain could interact with these and/or other surface functionalities on the cross-linked micelle. Small sugar products are not expected to benefit from such interactions.

One advantage of MINP(**7**+**8f**) was its well-defined catalytic site and improved mass transfer in the homogeneous reaction mixture. Recovery of homogeneous catalysts is often an associated problem. In the MINP preparation, the surface–core doubly cross-linked micelles were typically covered with monoazide **3** for enhanced hydrophilicity and facile purification (Scheme 1). Without the termination, the alkyne-containing MINPs could be easily "clicked" onto azide-functionalized magnetic nanoparticles (MNPs) prepared via a literature procedure[70] (Scheme S3). The resulting MINP(**7**+**8f**)@MNP composite (Figure 5) became a reusable heterogeneous catalyst that could be recovered simply with a magnet after each hydrolytic cycle. Figure 6 shows that the catalyst maintained 75% of its activity after 10 cycles of hydrolysis.
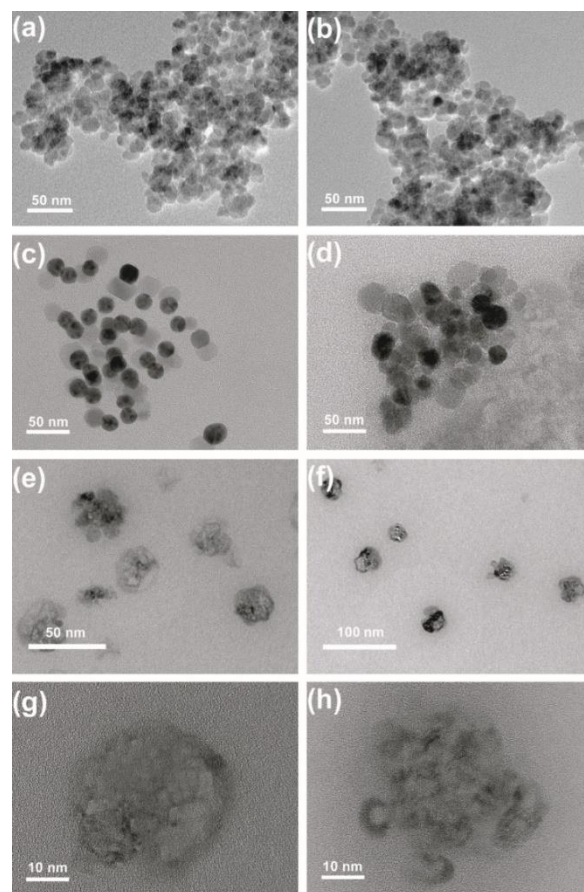

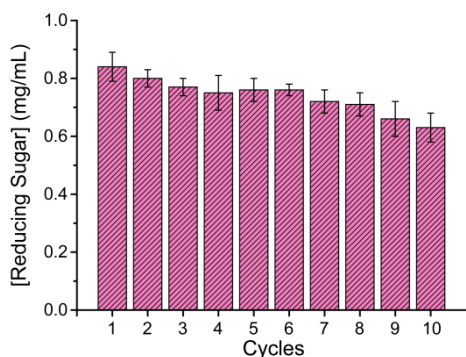**Figure 5.** TEM images of (a, b) silica gel-coated Fe$_3$O$_4$ magnetic nanoparticles, (c, d) NH$_2$-MNP, (e-h) the final MINP(**7**+**8f**)@MNP.

Figure 6. Recyclability of MINP(**7+8f**)@MNP for cellulose hydrolysis in 2:8 [C$_2$mim]OAc/DMSO with 5% H$_2$O at 90 °C.

CONCLUSIONS

In summary, micellar imprinting using judiciously designed templates and postmodification provide a powerful way to construct synthetic enzymes in a bottom-up fashion. What was key to the construction was the strong templating effect exemplified by the large imprint/nonimprint ratio (Table 2), nanodimension of the imprinted micelle, good accessibility of the imprinted pocket, and good solubility of MINP in solvents such as DMF and DMSO. These features allowed a facile one-pot synthesis of complex imprinted pockets from small-molecule template molecules in the core of water-soluble organic nanoparticles. In addition, they enabled chemical derivatization of the imprinted pockets by standard chemical reactions to convert them into synthetic enzymes with accurately positioned, tunable catalytic groups.

MINP(**7+8f**) came close to some natural β-glucosidases in the ability to hydrolyze cellobiose in aqueous solution and could function under conditions completely impossible for natural enzymes such as 83% H$_3$PO$_4$ and ionic liquids/DMSO mixture at 90 °C. The enzyme activity of 0.719 μmol mg^{-1} h^{-1} in 2:8 [C$_2$mim]OAc/DMSO with 5% H$_2$O was unprecedented for a synthetic glycosidase. A concoction of enzymes are often used by nature and also in industrial processes to hydrolyze cellulose—endocellulase to target the amorphous region of cellulose fibers, exocellulase to depolymerize the chain from the nonreducing end into glucose oligomers, and β-glucosidase to hydrolyze the oligomers.[29] It is envisioned that multiple synthetic mimics of these enzymes could work synergistically likewise, in aqueous and nonaqueous solutions where natural enzymes could not operate. Not only can the operating window of cellulose depolymerization be greatly expanded in such a way, the excellent reusability of the synthetic enzymes also represents another major advantage.

ASSOCIATED CONTENT

Supporting Information

Synthetic procedures, characterization of compounds and materials, ITC binding curves, additional tables and figures, and NMR data. This material is available free of charge via the Internet at http://pubs.acs.org.

AUTHOR INFORMATION

Corresponding Author

zhaoy@iastate.edu

ORCID

Xiaowei Li: 0000-0001-9479-4857
Milad Zangiabadi: 0000-0003-0886-1553
Yan Zhao: 0000-0003-1215-2565

REFERENCES

(1) Breslow, R. *Artificial Enzymes*; Wiley-VCH: Weinheim, 2005.
(2) Kirby, A. J.; Hollfelder, F. *From Enzyme Models to Model Enzymes*; Royal Society of Chemistry: Cambridge, UK, 2009.
(3) Raynal, M.; Ballester, P.; Vidal-Ferran, A.; van Leeuwen, P. W. N. M. Supramolecular Catalysis. Part 2: Artificial Enzyme Mimics. *Chem. Soc. Rev.* **2014**, *43*, 1734-1787.
(4) Knowles, J. R. Enzyme Catalysis: Not Different, Just Better. *Nature* **1991**, *350*, 121-124.
(5) Wulff, G. Enzyme-Like Catalysis by Molecularly Imprinted Polymers. *Chem. Rev.* **2002**, *102*, 1-28.
(6) Haupt, K.; Mosbach, K. Molecularly Imprinted Polymers and Their Use in Biomimetic Sensors. *Chem. Rev.* **2000**, *100*, 2495-2504.
(7) Ye, L.; Mosbach, K. Molecular Imprinting: Synthetic Materials as Substitutes for Biological Antibodies and Receptors. *Chem. Mater.* **2008**, *20*, 859-868.
(8) Pan, J.; Chen, W.; Ma, Y.; Pan, G. Molecularly Imprinted Polymers as Receptor Mimics for Selective Cell Recognition. *Chem. Soc. Rev.* **2018**, *47*, 5574-5587.
(9) Zhang, H. Molecularly Imprinted Nanoparticles for Biomedical Applications. *Adv. Mater.* **2020**, *32*, 1806328.
(10) Wulff, G.; Liu, J. Design of Biomimetic Catalysts by Molecular Imprinting in Synthetic Polymers: The Role of Transition State Stabilization. *Acc. Chem. Res.* **2012**, *45*, 239-247.
(11) Muratsugu, S.; Shirai, S.; Tada, M. Recent Progress in Molecularly Imprinted Approach for Catalysis. *Tetrahedron Lett.* **2020**, *61*, 151603.
(12) Kirsch, N.; Hedin-Dahlström, J.; Henschel, H.; Whitcombe, M. J.; Wikman, S.; Nicholls, I. A. Molecularly Imprinted Polymer Catalysis of a Diels-Alder Reaction. *J. Mol. Catal. B: Enzym.* **2009**, *58*, 110-117.
(13) Chen, Z. Y.; Xu, L.; Liang, Y.; Zhao, M. P. pH-Sensitive Water-Soluble Nanospheric Imprinted Hydrogels Prepared as Horseradish Peroxidase Mimetic Enzymes. *Adv. Mater.* **2010**, *22*, 1488-1492.
(14) Servant, A.; Haupt, K.; Resmini, M. Tuning Molecular Recognition in Water-Soluble Nanogels with Enzyme-Like Activity for the Kemp Elimination. *Chem.-Eur. J.* **2011**, *17*, 11052-11059.
(15) Shen, X.; Huang, C.; Shinde, S.; Jagadeesan, K. K.; Ekström, S.; Fritz, E.; Sellergren, B. Catalytic Formation of Disulfide Bonds in Peptides by Molecularly Imprinted Microgels at Oil/Water Interfaces. *ACS Appl. Mater. Interfaces* **2016**, *8*, 30484-30491.
(16) Yuan, Y.; Yang, Y.; Faheem, M.; Zou, X.; Ma, X.; Wang, Z.; Meng, Q.; Wang, L.; Zhao, S.; Zhu, G. Molecularly Imprinted Porous Aromatic Frameworks Serving as Porous Artificial Enzymes. *Adv. Mater.* **2018**, *30*, 1800069.
(17) Awino, J. K.; Zhao, Y. Protein-Mimetic, Molecularly Imprinted Nanoparticles for Selective Binding of Bile Salt Derivatives in Water. *J. Am. Chem. Soc.* **2013**, *135*, 12552-12555.
(18) Chen, K.; Zhao, Y. Effects of Nano-Confinement and Conformational Mobility on Molecular Imprinting of Cross-Linked Micelles. *Org. Biomol. Chem.* **2019**, *17*, 8611-8617.
(19) Duan, L.; Zangiabadi, M.; Zhao, Y. Synthetic Lectins for Selective Binding of Glycoproteins in Water. *Chem. Commun.* **2020**, *56*, 10199-10202.
(20) Zangiabadi, M.; Zhao, Y. Molecularly Imprinted Polymeric Receptors with Interfacial Hydrogen Bonds for Peptide Recognition in Water. *ACS Appl. Polym. Mater.* **2020**, *2*, 3171-3180.
(21) Awino, J. K.; Gunasekara, R. W.; Zhao, Y. Sequence-Selective Binding of Oligopeptides in Water through Hydrophobic Coding. *J. Am. Chem. Soc.* **2017**, *139*, 2188-2191.

(22) Arifuzzaman, M.; Zhao, Y. Artificial Zinc Enzymes with Fine-Tuned Catalytic Active Sites for Highly Selective Hydrolysis of Activated Esters. *ACS Catal.* **2018**, *8*, 8154-8161.

(23) Li, X.; Zhao, Y. Chiral Gating for Size- and Shape-Selective Asymmetric Catalysis. *J. Am. Chem. Soc.* **2019**, *141*, 13749-13752.

(24) Hu, L.; Arifuzzaman, M. D.; Zhao, Y. Controlling Product Inhibition through Substrate-Specific Active Sites in Nanoparticle-Based Phosphodiesterase and Esterase. *ACS Catal.* **2019**, *9*, 5019-5024.

(25) Bose, I.; Zhao, Y. pH-Controlled Nanoparticle Catalysts for Highly Selective Tandem Henry Reaction from Mixtures. *ACS Catal.* **2020**, *10*, 13973-13977.

(26) Huber, G. W.; Iborra, S.; Corma, A. Synthesis of Transportation Fuels from Biomass: Chemistry, Catalysts, and Engineering. *Chem. Rev.* **2006**, *106*, 4044-4098.

(27) Luterbacher, J. S.; Martin Alonso, D.; Dumesic, J. A. Targeted Chemical Upgrading of Lignocellulosic Biomass to Platform Molecules. *Green Chem.* **2014**, *16*, 4816-4838.

(28) Jing, Y.; Guo, Y.; Xia, Q.; Liu, X.; Wang, Y. Catalytic Production of Value-Added Chemicals and Liquid Fuels from Lignocellulosic Biomass. *Chem* **2019**, *5*, 2520-2546.

(29) Payne, C. M.; Knott, B. C.; Mayes, H. B.; Hansson, H.; Himmel, M. E.; Sandgren, M.; Ståhlberg, J.; Beckham, G. T. Fungal Cellulases. *Chem. Rev.* **2015**, *115*, 1308-1448.

(30) Wahlström, R. M.; Suurnäkki, A. Enzymatic Hydrolysis of Lignocellulosic Polysaccharides in the Presence of Ionic Liquids. *Green Chem.* **2015**, *17*, 694-714.

(31) Brogan, A. P. S.; Bui-Le, L.; Hallett, J. P. Non-Aqueous Homogenous Biocatalytic Conversion of Polysaccharides in Ionic Liquids Using Chemically Modified Glucosidase. *Nat. Chem.* **2018**, *10*, 859-865.

(32) Wulff, G.; Vesper, W. Enzyme-Analogue Built Polymers .8. Preparation of Chromatographic Sorbents with Chiral Cavities for Racemic-Resolution. *J. Chromatogr.* **1978**, *167*, 171-186.

(33) James, T. D.; Phillips, M. D.; Shinkai, S. *Boronic Acids in Saccharide Recognition*; RSC Publishing: Cambridge, 2006.

(34) Pal, A.; Bérubé, M.; Hall, D. G. Design, Synthesis, and Screening of a Library of Peptidyl Bis(Boroxoles) as Oligosaccharide Receptors in Water: Identification of a Receptor for the Tumor Marker TF-Antigen Disaccharide. *Angew. Chem. Int. Ed.* **2010**, *49*, 1492-1495.

(35) Li, X.; Zhao, Y. Synthetic Glycosidase Distinguishing Glycan and Glycosidic Linkage in Its Catalytic Hydrolysis. *ACS Catal.* **2020**, *10*, 13800-13808.

(36) Dowlut, M.; Hall, D. G. An Improved Class of Sugar-Binding Boronic Acids, Soluble and Capable of Complexing Glycosides in Neutral Water. *J. Am. Chem. Soc.* **2006**, *128*, 4226-4227.

(37) Kim, H.; Kang, Y. J.; Kang, S.; Kim, K. T. Monosaccharide-Responsive Release of Insulin from Polymersomes of Polyboroxole Block Copolymers at Neutral pH. *J. Am. Chem. Soc.* **2012**, *134*, 4030-4033.

(38) Gunasekara, R. W.; Zhao, Y. A General Method for Selective Recognition of Monosaccharides and Oligosaccharides in Water. *J. Am. Chem. Soc.* **2017**, *139*, 829-835.

(39) Li, X.; Zhao, Y. Synthetic Glycosidases for the Precise Hydrolysis of Oligosaccharides and Polysaccharides. *Chem. Sci.* **2021**, *12*, 374-383.

(40) Bérubé, M.; Dowlut, M.; Hall, D. G. Benzoboroxoles as Efficient Glycopyranoside-Binding Agents in Physiological Conditions: Structure and Selectivity of Complex Formation. *J. Org. Chem.* **2008**, *73*, 6471-6479.

(41) Xing, X.; Zhao, Y. Binding-Promoted Chemical Reaction in the Nanospace of a Binding Site: Effects of Environmental Constriction. *Org. Biomol. Chem.* **2018**, *16*, 2855-2859.

(42) Xing, X.; Zhao, Y. Fluorescent Nanoparticle Sensors with Tailor-Made Recognition Units and Proximate Fluorescent Reporter Groups. *New J. Chem.* **2018**, *42*, 9377-9380.

(43) Zechel, D. L.; Withers, S. G. Glycosidase Mechanisms: Anatomy of a Finely Tuned Catalyst. *Acc. Chem. Res.* **2000**, *33*, 11-18.

(44) Toone, E. J. Structure and Energetics of Protein-Carbohydrate Complexes. *Curr. Opin. Struct. Biol.* **1994**, *4*, 719-728.

(45) Fife, T. H.; Jao, L. K. Substituent Effects in Acetal Hydrolysis. *J. Org. Chem.* **1965**, *30*, 1492-1495.

(46) *CRC Handbook of Chemistry and Physics*; 88th ed.; Lide, D. R. Ed. CRC Press/Taylor & Francis Group: Boca Raton, FL, 2007; p8-42.

(47) Westheimer, F. H. Coincidences, Decarboxylation, and Electrostatic Effects. *Tetrahedron* **1995**, *51*, 3-20.

(48) Matulis, D.; Bloomfield, V. A. Thermodynamics of the Hydrophobic Effect. I. Coupling of Aggregation and pK_a Shifts in Solutions of Aliphatic Amines. *Biophys. Chem.* **2001**, *93*, 37-51.

(49) Henao, J. D.; Suh, Y.-W.; Lee, J.-K.; Kung, M. C.; Kung, H. H. Striking Confinement Effect: AuCl$_4^-$ Binding to Amines in a Nanocage Cavity. *J. Am. Chem. Soc.* **2008**, *130*, 16142-16143.

(50) Bose, I.; Fa, S.; Zhao, Y. Tunable Artificial Enzyme–Cofactor Complex for Selective Hydrolysis of Acetals. *J. Org. Chem.* **2021**, *86*, 1701-1711.

(51) Tomsho, J. W.; Pal, A.; Hall, D. G.; Benkovic, S. J. Ring Structure and Aromatic Substituent Effects on the pK_a of the Benzoxaborole Pharmacophore. *ACS Med. Chem. Lett.* **2012**, *3*, 48-52.

(52) Mohd Shafie, Z.; Yu, Y.; Wu, H. Effect of Initial Ph on Hydrothermal Decomposition of Cellobiose under Weakly Acidic Conditions. *Fuel* **2015**, *158*, 315-321.

(53) Singhania, R. R.; Patel, A. K.; Pandey, A.; Ganansounou, E. Genetic Modification: A Tool for Enhancing Beta-Glucosidase Production for Biofuel Application. *Bioresour. Technol.* **2017**, *245*, 1352-1361.

(54) Sun, J.; Wang, W.; Ying, Y.; Hao, J. A Novel Glucose-Tolerant Gh1 B-Glucosidase and Improvement of Its Glucose Tolerance Using Site-Directed Mutation. *Appl. Biochem. Biotechnol.* **2020**, *192*, 999-1015.

(55) Tamaki, F. K.; Araujo, É. M.; Rozenberg, R.; Marana, S. R. A Mutant B-Glucosidase Increases the Rate of the Cellulose Enzymatic Hydrolysis. *Biochem. Biophys. Rep.* **2016**, *7*, 52-55.

(56) Okada, G. Cellulase of *Aspergillus Niger*. *Meth. Enzymol.* **1988**, *160*, 259-264.

(57) Jurick Ii, W. M. Application of the 2-Cyanoacetamide Method for Spectrophotometric Assay of Cellulase Enzyme Activity. *Plant Pathol. J.* **2012**, *11*, 38-41.

(58) Igarashi, K.; Uchihashi, T.; Koivula, A.; Wada, M.; Kimura, S.; Okamoto, T.; Penttilä, M.; Ando, T.; Samejima, M. Traffic Jams Reduce Hydrolytic Efficiency of Cellulase on Cellulose Surface. *Science* **2011**, *333*, 1279-1282.

(59) Payne, C. M.; Jiang, W.; Shirts, M. R.; Himmel, M. E.; Crowley, M. F.; Beckham, G. T. Glycoside Hydrolase Processivity Is Directly Related to Oligosaccharide Binding Free Energy. *J. Am. Chem. Soc.* **2013**, *135*, 18831-18839.

(60) Nakamura, A.; Watanabe, H.; Ishida, T.; Uchihashi, T.; Wada, M.; Ando, T.; Igarashi, K.; Samejima, M. Trade-Off between Processivity and Hydrolytic Velocity of Cellobiohydrolases at the Surface of Crystalline Cellulose. *J. Am. Chem. Soc.* **2014**, *136*, 4584-4592.

(61) Zhang, Y. H. P.; Cui, J.; Lynd, L. R.; Kuang, L. R. A Transition from Cellulose Swelling to Cellulose Dissolution by O-Phosphoric Acid: Evidence from Enzymatic Hydrolysis and Supramolecular Structure. *Biomacromolecules* **2006**, *7*, 644-648.

(62) Wang, H.; Gurau, G.; Rogers, R. D. Ionic Liquid Processing of Cellulose. *Chem. Soc. Rev.* **2012**, *41*, 1519-1537.

(63) Swatloski, R. P.; Spear, S. K.; Holbrey, J. D.; Rogers, R. D. Dissolution of Cellose with Ionic Liquids. *J. Am. Chem. Soc.* **2002**, *124*, 4974-4975.

(64) Rinaldi, R.; Palkovits, R.; Schuth, F. Depolymerization of Cellulose Using Solid Catalysts in Ionic Liquids. *Angew. Chem. Int. Ed.* **2008**, *47*, 8047-8050.

(65) Binder, J. B.; Raines, R. T. Fermentable Sugars by Chemical Hydrolysis of Biomass. *Proc. Natl. Acad. Sci. U. S. A.* **2010**, *107*, 4516-4521.

(66) Zhang, Z.; Song, J.; Han, B. Catalytic Transformation of Lignocellulose into Chemicals and Fuel Products in Ionic Liquids. *Chem. Rev.* **2017**, *117*, 6834-6880.

(67) Rinaldi, R. Instantaneous Dissolution of Cellulose in Organic Electrolyte Solutions. *Chem. Commun.* **2011**, *47*, 511-513.

(68) de Oliveira, H. F. N.; Farès, C.; Rinaldi, R. Beyond a Solvent: The Roles of 1-Butyl-3-Methylimidazolium Chloride in the Acid-Catalysis for Cellulose Depolymerisation. *Chem. Sci.* **2015**, *6*, 5215-5224.

(69) Turner, M. B.; Spear, S. K.; Huddleston, J. G.; Holbrey, J. D.; Rogers, R. D. Ionic Liquid Salt-Induced Inactivation and Unfolding of Cellulase from Trichoderma Reesei. *Green Chem.* **2003**, *5*, 443-447.

(70) Lin, P.-C.; Chou, P.-H.; Chen, S.-H.; Liao, H.-K.; Wang, K.-Y.; Chen, Y.-J.; Lin, C.-C. Ethylene Glycol-Protected Magnetic Nanoparticles for a Multiplexed Immunoassay in Human Plasma. *Small* **2006**, *2*, 485-489.

cellulose

glucose yield

synthetic glucosidase in DMSO + ionic liquid at 90 °C

natural cullulase in aqueous buffer at 37 °C

time